

Contents lists available at [ScienceDirect](https://www.sciencedirect.com)

## Deep-Sea Research Part I

journal homepage: [www.elsevier.com/locate/dsri](http://www.elsevier.com/locate/dsri)

## Near 7-day response of ocean bottom pressure to atmospheric surface pressure and winds in the northern South China Sea

Kun Zhang<sup>a</sup>, Xiao-Hua Zhu<sup>a,b,\*</sup>, Ruixiang Zhao<sup>a</sup><sup>a</sup> State Key Laboratory of Satellite Ocean Environment Dynamics, Second Institute of Oceanography, State Oceanic Administration, Hangzhou 310012, China<sup>b</sup> Ocean College, Zhejiang University, Hangzhou 310058, China

## ARTICLE INFO

## Keywords:

Ocean bottom pressure  
 Pressure-recording inverted echo sounder  
 Atmospheric surface pressure  
 Winds  
 Ekman pumping/suction  
 South China Sea

## ABSTRACT

Ocean bottom pressures, observed by five pressure-recording inverted echo sounders (PIESs) from October 2012 to July 2014, exhibit strong near 7-day variability in the northern South China Sea (SCS) where long-term in situ bottom pressure observations are quite sparse. This variability was strongest in October 2013 during the near two years observation period. By joint analysis with European Center for Medium-Range Weather Forecasts (ECMWF) data, it is shown that the near 7-day ocean bottom pressure variability is closely related to the local atmospheric surface pressure and winds. Within a period band near 7 days, there are high coherences, exceeding 95% significance level, of observed ocean bottom pressure with local atmospheric surface pressure and with both zonal and meridional components of the wind. Ekman pumping/suction caused by the meridional component of the wind in particular, is suggested as one driving mechanism. A Kelvin wave response to the near 7-day oscillation would propagate down along the continental slope, observed at the Qui Nhon in the Vietnam. By multiple and partial coherence analyses, we find that local atmospheric surface pressure and Ekman pumping/suction show nearly equal influence on ocean bottom pressure variability at near 7-day periods. A schematic diagram representing an idealized model gives us a possible mechanism to explain the relationship between ocean bottom pressure and local atmospheric forcing at near 7-day periods in the northern SCS.

## 1. Introduction

Ocean bottom pressure ( $P_{\text{bot}}$ ) is a fundamental measure in understanding oceanographic progresses (Eble and Gonzalez, 1991; Quinn and Ponte, 2011). However, long-term in situ bottom pressure measurements lasting more than a year are sparse (Hirose et al., 2001; Na et al., 2012) resulting in poor understanding of  $P_{\text{bot}}$  variability. The Gravity Recovery and Climate Experiment (GRACE) satellites were launched in 2002 to measure variability of global gravity and  $P_{\text{bot}}$  with 1-month interval. But the temporal sample resolution is too low to catch higher frequency variability of  $P_{\text{bot}}$  (Quinn and Ponte, 2011; Na et al., 2012). Furthermore, as with the typical 10 day satellite altimeter sample interval, the GRACE data 1-month interval can induce aliasing error (Gille and Hughes, 2001; Nam et al., 2004). Thus, it is an important mission to reduce the GRACE aliasing error (Wiese et al., 2009; Dobsław et al., 2013). Indeed, the accuracy of GRACE may be mainly limited by the fact of aliasing (Quinn and Ponte, 2011).

In early days, Luther (1982) disclosed a barotropic planetary oscillation with 4–6 day periods in the Pacific Ocean. During the North Pacific Barotropic Electromagnetic and Pressure Experiment (BEMPEX),

predecessors had observed that  $P_{\text{bot}}$  was related to large-scale atmospheric surface pressure ( $P_{\text{atm}}$ ) with periods longer than 10 days (Luther et al., 1990). Ponte (1997) demonstrated, through numerical experiments, that 5-day nonisostatic response of the global ocean is driven by Rossby-Haurwitz waves in  $P_{\text{atm}}$ . Observations confirmed the simulation using several long-term sub-surface and bottom pressure measurements in the Atlantic Ocean (Park and Watts, 2006). Recently, Na et al. (2012) found near 13-day barotropic ocean response to atmospheric forcing in the Kuroshio Extension System Study (KESS) by utilizing in situ bottom pressure measurements derived from pressure-recording inverted echo sounders (PIESs) deployed for about 2 years. The variability of  $P_{\text{bot}}$  at periods between 7 and 60 days is principally driven by an atmospheric mode and an oceanic mode (Na et al., 2016). Furthermore, Na et al. (2016) demonstrated that the atmospheric mode becomes more important with decreasing periods from 60 to 7 days.

In particular, the inverted barometer (IB) response is an isostatic adjustment of sea level to change in barometric pressure, in the case of full adjustment, an increase (decrease) in  $P_{\text{atm}}$  of 1 hPa corresponds to a decrease (increase) in sea level of about 1 cm, which means the observed pressures at sea bottom are unchanged (Brown et al., 1975;

\* Corresponding author at: State Key Laboratory of Satellite Ocean Environment Dynamics, Second Institute of Oceanography, State Oceanic Administration, Hangzhou 310012, China.  
 E-mail address: [xhzhz@sio.org.cn](mailto:xhzhz@sio.org.cn) (X.-H. Zhu).

<https://doi.org/10.1016/j.dsr.2017.12.004>

Received 18 June 2017; Received in revised form 31 October 2017  
 0967-0637/ © 2017 Elsevier Ltd. All rights reserved.

Wunsch and Stammer, 1997). Predecessors have found that IB response generally occurs in the open ocean at periods between 2 and 30 days (Brown et al., 1975; Mathers and Woodworth, 2001). However, many studies have demonstrated non-IB response near 5-day periods resulting from Rossby-Haurwitz waves, a westward propagating global-scale oscillation in  $P_{\text{atm}}$  with period near 5 days (Madden and Julian, 1972; Woodworth et al., 1995; Ponte, 1997; Park and Watts, 2006). Furthermore, nonisostatic response to  $P_{\text{atm}}$  at other periods also has been observed in some special sea areas, such as about 2–7 days in the semi-enclosed Japan Sea (Park and Watts, 2005), and near 13 days in the Kuroshio Extension (Na et al., 2012).

Compared with  $P_{\text{atm}}$ , winds play an important role in sea surface height variability which is directly linked to  $P_{\text{bot}}$  (Ponte, 1994; Fu, 2003; Andres et al., 2012). Previous research has shown that local winds are a major factor driving  $P_{\text{bot}}$  variability at periods shorter than 10 days, whereas large-scale winds can affect  $P_{\text{bot}}$  variability at some longer periods (Willebrand et al., 1980; Luther et al., 1990; Na et al., 2012). In the Kuroshio Extension, there is good negative correlation between wind stress curl and  $P_{\text{bot}}$  at periods near 13 days which is possibly caused by Ekman suction (divergence) and pumping (convergence) (Na et al., 2012). Indeed, Ekman pumping/suction is an important indicator of sea level variability (Rong et al., 2007; Wang et al., 2011). Petrick et al. (2014) found variability of  $P_{\text{bot}}$  is related both to  $P_{\text{atm}}$  and to winds in the North Pacific through two modes.

The South China Sea (SCS) is one of the largest semi-enclosed ocean basins located between the Pacific and Indian Oceans. It has an average depth of about 2000 m, and a maximum depth of about 5000 m. At the northeast boundary of the SCS there are two important straits, the Taiwan Strait and the Luzon Strait (Xiao et al., 2016). The Tibetan Plateau is located northwest of the SCS where the near 7-day atmosphere oscillation, propagating southeastward, was reported (Xie et al., 1989). Despite the SCS being an important marginal sea of the North Pacific Ocean, there have been few studies of  $P_{\text{bot}}$  variability based on in situ measurements in it. Theory and observations in the Japan Sea, another large semi-enclosed ocean basin, have shown a nonisostatic response of  $P_{\text{bot}}$  to  $P_{\text{atm}}$  variations (Lyu et al., 2002; Park and Watts, 2005). However,  $P_{\text{bot}}$  variability and its causes are unknown in the northern SCS. The aim of our paper is to address these issues; it is organized as follows. Section 2 describes the data and processing methods used in this study. Section 3 examines the near 7-day  $P_{\text{bot}}$  variability in the northern SCS and its relationship with  $P_{\text{atm}}$  and winds. Section 4 describes a possible mechanism to explain the relationship and account for mutual and partial coherences between influential inputs.

## 2. Data and methods

The  $P_{\text{bot}}$  data were measured by five PIESs which were deployed from October 2012 to July 2014 in the northern SCS (Fig. 1, Table 1, Fig. 2a) (Zhu et al., 2015; Zhao et al., 2016; Zhao and Zhu, 2016). Each PIES instrument was equipped with a high-resolution pressure gauge which can measure ocean bottom pressure with absolute accuracy of  $\pm 0.01\%$  and resolution of 0.1 mbar (Inverted Echo Sounder User's Manual, <http://www.po.gso.uri.edu/dynamics/IES/index.html>). Following Kennelly et al. (2007) and Park et al. (2012), the  $P_{\text{bot}}$  records were despiked, detided and dedrifted. First, the  $P_{\text{bot}}$  records were despiked to reject measurement spikes. Then, diurnal and semi-diurnal tidal signals were determined and subtracted from all of the  $P_{\text{bot}}$  records using response-method tidal analysis (Munk and Cartwright, 1966). Finally, pressure drift was also eliminated by the method of least-squares. Moreover, the recorded times of  $P_{\text{bot}}$  measurement were converted to UTC time. The results from variance-preserving power spectral density analysis of the  $P_{\text{bot}}$  records are shown in Fig. 3a; clear peaks can be seen at periods of 4.3, 7.4 and 14.6 days. In this study, we are only concerned with the near 7-day period band. In order to extract signals of interest to us in this study, a 3rd-order Butterworth band-pass filter with cutoff periods of 6.5 and 8.5 days was applied to the  $P_{\text{bot}}$

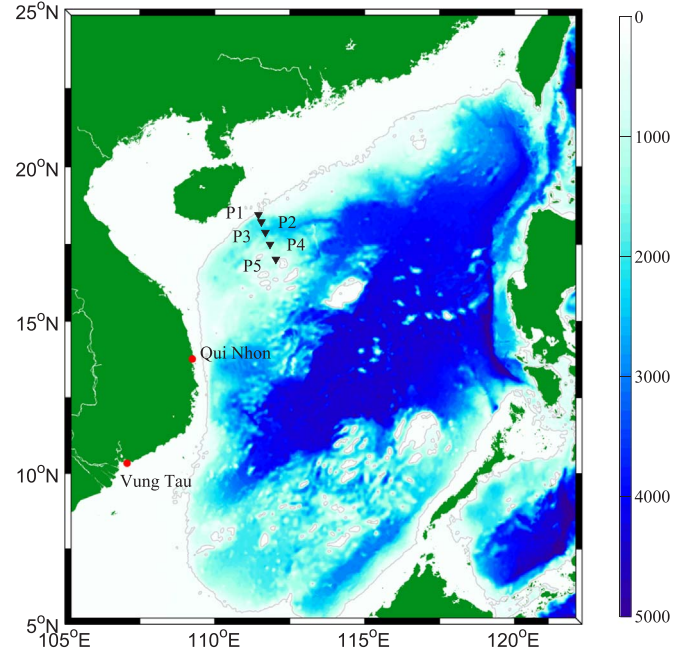


Fig. 1. Map of the South China Sea. Black triangles (P1, P2, P3, P4 and P5) and red dots indicate PIES stations and tide gauges, respectively. Color contours show bathymetry in meters. Gray lines indicate isobaths of 200 m. (For interpretation of the references to color in this figure legend, the reader is referred to the web version of this article.)

Table 1  
Information on PIES sites.

PIES number	P1	P2	P3	P4	P5
Longitude (°E)	111.45	111.55	111.69	111.84	112.04
Latitude (°N)	18.45	18.22	17.88	17.49	17.01
Depth (m)	642	1842	2091	1348	1030
Observation period	Oct. 2012–Jul. 2014				
Measurement interval	1 h				

records (Fig. 2b).

In order to investigate the cause of the 7.4 day peak in the variance-preserving power spectra (Fig. 3a), we utilized data of  $P_{\text{atm}}$  and 10 m wind velocity, obtained from the European Center for Medium-Range Weather Forecasts (ECMWF) (available at <http://www.ecmwf.int/>). The spatial resolution is  $0.75^\circ \times 0.75^\circ$ , and the temporal interval is 6 h. We applied the same Butterworth band-pass filter to the ECMWF data (Fig. 2d, f). To analyze the effect of winds on  $P_{\text{bot}}$ , we calculated the Ekman transport per unit width in the Ekman layer at every grid point through the following method (Smith, 1968; Talley et al., 2011):

$$\vec{U}_E = \int \vec{v}(z) dz = \frac{1}{\rho f} (\vec{\tau} \times \vec{\kappa}) \quad (1)$$

$$\vec{\tau} = K_z \cdot \rho_{\text{air}} \cdot \vec{V}_{10} \cdot |\vec{V}_{10}| \quad (2)$$

where  $\vec{U}_E$  is the associated Ekman transport, which has units of depth times velocity, hence  $\text{m}^2/\text{s}$ , rather than area times velocity.  $\rho$  is the density of seawater, which is assumed constant with a value of  $1024 \text{ kg/m}^3$ .  $f$  is the Coriolis parameter.  $\vec{\tau}$  is the wind stress vector (calculated by Eq. (2)).  $\vec{\kappa}$  is a unit vector normal to the sea surface upward.  $\vec{v}$  is Ekman horizontal velocity in the Ekman layer.  $K_z$  is a bulk transfer coefficient for momentum (typically  $1.5 \times 10^{-3} \text{ m}^2/\text{s}$ ).  $\rho_{\text{air}}$  is the density of air at the surface, which is assumed constant with a value of  $1.225 \text{ kg/m}^3$ .  $\vec{V}_{10}$  is the wind velocity at a height of 10 m. The vertical velocity  $w_E$  (Ekman pumping/suction velocity) at the base of the Ekman layer is also calculated:

Download English Version:

<https://daneshyari.com/en/article/8884272>

Download Persian Version:

<https://daneshyari.com/article/8884272>

[Daneshyari.com](https://daneshyari.com)